

## Nuclear Order in Copper: New Type of Antiferromagnetism in an Ideal fcc System

A. J. Annala,<sup>(1)</sup> K. N. Clausen,<sup>(2)</sup> P.-A. Lindgård,<sup>(2)</sup> O. V. Lounasmaa,<sup>(1)</sup> A. S. Oja,<sup>(1)</sup>  
K. Siemensmeyer,<sup>(3),(a)</sup> M. Steiner,<sup>(3),(a)</sup> J. T. Tuoriniemi,<sup>(1)</sup> and H. Weinfurter<sup>(3)</sup>

<sup>(1)</sup>Low Temperature Laboratory, Helsinki University of Technology, SF-02150 Espoo, Finland

<sup>(2)</sup>Physics Department, Risø National Laboratory, DK-4000 Roskilde, Denmark

<sup>(3)</sup>Hahn-Meitner Institut, D-1000 Berlin 39, Federal Republic of Germany

(Received 2 January 1990)

A new ordering vector  $\mathbf{k} = (2\pi/a)(0, \frac{2}{3}, \frac{2}{3})$  for the fcc antiferromagnets has been found by neutron-diffraction experiments at nanokelvin temperatures in the nuclear-spin system of a  $^{65}\text{Cu}$  single crystal. The corresponding reflection, together with the previously observed (100) Bragg peak, shows the presence of three antiferromagnetic phases, separated by two first-order phase transitions, as the external magnetic field is varied between zero and  $B_c = 0.25$  mT. The kinetics of the transitions was observed to be on the order of seconds.

PACS numbers: 75.25.+z, 07.20.Mc, 61.12.Gz, 75.50.Ee

A new magnetic structure has been found in the fcc antiferromagnets. By neutron-diffraction experiments, four equivalent nuclear magnetic Bragg reflections  $\pm(0\frac{2}{3}\frac{2}{3})$ ,  $(1\frac{1}{3}\frac{1}{3})$ , and  $(1-\frac{1}{3}-\frac{1}{3})$  have been observed in the spin system of a  $^{65}\text{Cu}$  single crystal. It was unexpected that the ordering proved to be simply commensurate with the lattice, corresponding to a structure with three sublattices. The discoveries were made when the reciprocal space was searched along high-symmetry directions. This is the first time that conventional scanning has been employed at nanokelvin temperatures.

Magnetic ordering in copper has evoked considerable experimental and theoretical interest over the past decade. Nuclear antiferromagnetism in an elemental metal was observed, for the first time, by means of low-frequency ac susceptibility measurements on a polycrystalline copper sample.<sup>1</sup> Subsequent experiments on a single crystal showed the presence of three different antiferromagnetic regions as a function of the external magnetic field, aligned along the [001] direction.<sup>2</sup>

This was surprising and, in order to determine the different spin structures, neutron-diffraction experiments were initiated.<sup>3</sup> The spin dependence of the nuclear neutron-scattering cross section<sup>4,5</sup> enables investigations similar to those used in electronic magnetism. The isotropic nature of the nuclear scattering, however, makes it more difficult to determine the spin directions.

In the first neutron-diffraction experiments on copper<sup>6,7</sup> the external field was aligned along the [01 $\bar{1}$ ] direction, and the nuclear antiferromagnetic (100) Bragg peak,  $X$  (see Fig. 1), was observed in two distinct field regions, near  $B=0$  and around 0.15 mT. It was puzzling that no neutron intensity was found at  $B=0.10$  mT, even though the simultaneously measured longitudinal susceptibility indicated order at this field.

Nearest-neighbor interaction dominates in copper<sup>8</sup> and favors antiparallel spin alignment. Since in the fcc lattice all spins are fixed to the corners of rigid equilateral triangles, this is expected to cause "frustration."

The ground state of such a system is still one of the unsolved problems in magnetism.<sup>9,10</sup> The ordered spin structures of copper have been investigated recently by spin-wave theory,<sup>11</sup> by second-order perturbation theory for a cluster of spins,<sup>12</sup> and by Monte Carlo simulations.<sup>13,14</sup>

On the basis of first-principles calculations it has been shown<sup>8,15</sup> that the fundamental ordering vector is expected at  $X$ , but that another vector along  $\Gamma K$ ,  $(0, \eta, \eta)$  (see Fig. 1), is very close in energy,<sup>8</sup> in particular, if the strength of the Ruderman-Kittel interaction<sup>16</sup> relative to the dipolar force is slightly reduced from the experimental value.<sup>17,18</sup> Fluctuations could then stabilize a  $\Gamma K$  structure at the boundary between the two (100) phases.<sup>12,19</sup> An ordering vector along  $\Gamma X$ ,  $(\xi, 0, 0)$ , has

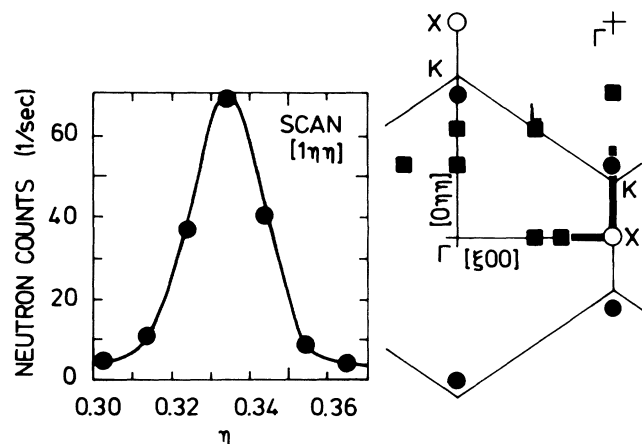


FIG. 1. Left: Neutron intensity vs position along  $\Gamma K$ ,  $[1\eta\eta]$ , showing the discovery of the  $(1\frac{1}{3}\frac{1}{3})$  Bragg reflection. Right: The  $(01\bar{1})$  scattering plane in the Brillouin zone of an fcc lattice. The search scans (for details see text) are marked with thick lines, the observed  $\pm(0\frac{2}{3}\frac{2}{3})$ ,  $(1\frac{1}{3}\frac{1}{3})$ , and  $(1-\frac{1}{3}-\frac{1}{3})$  reflections are indicated by ●, and the (100) reflections are shown by ○. No intensity was observed at the commensurate positions indicated by ■.

also been proposed.<sup>15,20,21</sup>

The extremely low nuclear ordering temperature in copper imposes severe experimental restrictions. The measuring time is limited because the spins can be adiabatically cooled below the Néel temperature,  $T_c = 58$  nK, only once every 36 h by means of nuclear demagnetization<sup>7</sup> and because the spin-lattice relaxation process warms up the nuclear-spin system to the paramagnetic region in about 5 min. Mechanical movements of the cryostat and the detector during scans contribute additional vibrational heat, thus further reducing the measuring time.

The cryostat has to be kept upright and this restricts the scans, with our present sample orientation, to the plane spanned by the  $[\xi 00]$  and  $[0\eta\eta]$  directions (see Fig. 1). The neutron wavelength  $\lambda = 4.7$  Å was found to give optimal signal-to-noise ratio and access to the symmetry lines of interest. Second- and third-order reflections from the monochromator were used to align the sample. During the experiments these were removed by a cooled BeO filter.

The search scans were performed as follows: Prior to nuclear demagnetization, the diffractometer was positioned at the starting point of the scan. We estimate that the polarization was  $0.96 \pm 0.01$ , just before entering the ordered state. When the chosen final field was reached, the neutron signal was monitored for about 10 sec, before moving to the next reciprocal-lattice position in a step equal to the half-width of the spectrometer resolution. As the scan proceeded and the nuclear spins warmed up, the counting times were increased to maintain sufficient counting statistics. The intervals of the high-symmetry lines and some additional commensurate points<sup>22</sup> which were investigated are shown in Fig. 1.

Our search for a new reflection was rewarded when a very clear Bragg peak was found at  $(1\eta\eta)$ , with  $\eta = 0.33 \pm 0.01$ , in the external field  $B = 0.07$  mT (see Fig. 1). Later the  $\pm(0\frac{2}{3}\frac{2}{3})$  and  $(1-\frac{1}{3}-\frac{1}{3})$  reflections were observed as well. All four points are equivalent under fcc symmetry. The order is, within experimental accuracy, commensurate with the lattice structure. In particular, the  $(0\frac{1}{3}\frac{1}{3})$  and  $(-\frac{1}{3}\frac{1}{3}\frac{1}{3})$  positions were carefully searched for over the whole region below the critical field  $B_c = 0.25$  mT, but no neutrons above the background were detected.

In order to determine the phase diagram, intensities of the  $(1\frac{1}{3}\frac{1}{3})$  and  $(100)$  reflections were measured at eighteen different external magnetic fields. This was done by monitoring the neutron signal as a function of time while the spin system was warming up at constant  $B$ ; the method is schematically illustrated in the inset of Fig. 2(a).

In Figs. 2(a)–2(c) we give three examples of warmup curves. Temperature, which can be determined only in the paramagnetic phase, is monotonically increasing with time in the ordered phase. Figure 2(a), with data mea-

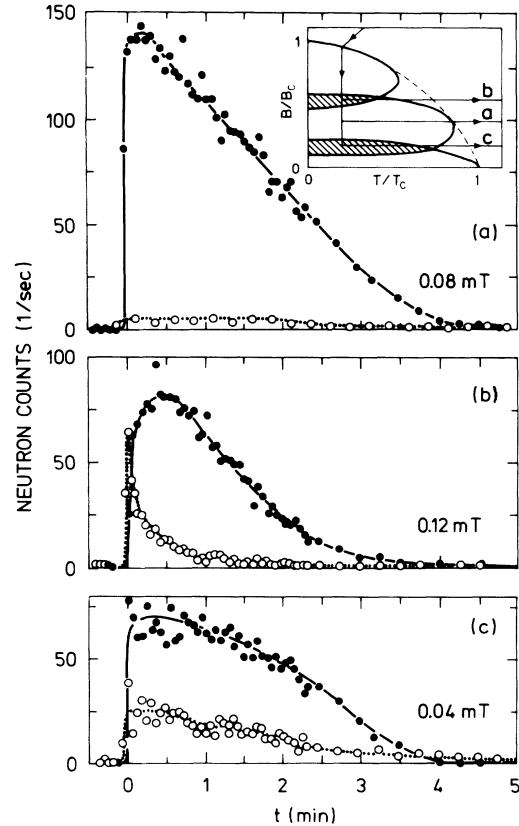


FIG. 2. (a) Time dependence of the  $(1\frac{1}{3}\frac{1}{3})$  reflection at  $B=0.08$  mT. Inset: A schematic phase diagram in the  $B$ - $T$  plane; the lines with arrows indicate entrance along an isentrope ( $S=0.15R\ln 4$ ) into the ordered phase and subsequent measurements in a constant field; and  $a$ ,  $b$ , and  $c$  correspond to the curves in parts (a), (b), and (c), respectively. (b) Time dependencies of the  $(1\frac{1}{3}\frac{1}{3})$  ( $\bullet$ ) and  $(100)$  ( $\circ$ ) reflections in the vicinity of the upper phase boundary. (c) Same for the lower phase boundary.

sured at  $B=0.08$  mT, shows how the  $(1\frac{1}{3}\frac{1}{3})$  neutron intensity decreases due to the warmup process.

The data presented in Figs. 2(b) and 2(c) illustrate the kinetics of the transitions. At  $B=0.12$  mT, the simultaneous disappearance of the  $(100)$  signal and appearance of the  $(1\frac{1}{3}\frac{1}{3})$  reflection indicate a first-order phase transition. At  $B=0.04$  mT, the  $(100)$  neutron intensity increases during the first minute, whereafter the  $(1\frac{1}{3}\frac{1}{3})$  and  $(100)$  peaks both decrease slowly during the next few minutes. This behavior could be explained by domain growth, which increases the intensity initially and tends to counteract the decrease caused by the warmup.<sup>23</sup>

The observed kinetics is a consequence of our demagnetization technique [see inset of Fig. 2(a)], which requires passage through the higher-field phase prior to entering the lower-field phase. During the passage, the upper phase is formed, and some seconds are needed for

it to disappear. This time scale is very convenient for further studies of kinetic effects in the spin system.<sup>24</sup>

From the neutron-count versus time curves a neutron intensity contour diagram was constructed; it is shown in Fig. 3. Three maxima occur: at  $B=0.09$  mT for the  $(\frac{1}{3}, \frac{1}{3})$  reflection, and at  $B=0$  and 0.15 mT for the (100) reflection. The  $(\frac{1}{3}, \frac{1}{3})$  signal is strongest when the (100) signal is weakest and vice versa, implying the presence of three distinct phases.

The upper phase boundary is at  $B \approx 0.12$  mT, where the contours in Fig. 3 are closely spaced. One can see how the neutron intensity moves, as a function of time, from one reflection to the other. Hysteresis was observed when the external magnetic field was repeatedly swept up and down across the transition region.

At the boundary between the uppermost and the middle phases, the outer contours of the  $(\frac{1}{3}, \frac{1}{3})$  and (100) signals both bend strongly inwards before crossing. The lower transition from the  $(\frac{1}{3}, \frac{1}{3})$  peak back to the (100) reflection takes place over a wide field region. The  $(\frac{1}{3}, \frac{1}{3})$  signal shows rapid disappearance only below  $B=0.02$  mT, whereas the (100) intensity begins to grow already at 0.07 mT. Between these fields both peaks are clearly visible simultaneously, but with different time evolutions. This we consider as evidence for the coexistence of two phases. All experimental data are thus consistent with both transitions being of first order.

In the narrow interval from  $B=0.02$  to 0.05 mT, a two- $\mathbf{k}$  phase, with two simultaneous ordering vectors, cannot be excluded since the temporal behavior of the  $(\frac{1}{3}, \frac{1}{3})$  and (100) peaks is similar.

In order to see the largest antiferromagnetic signal as a function of the external field, a cut of the contour diagram of Fig. 3 through the three maxima is shown in

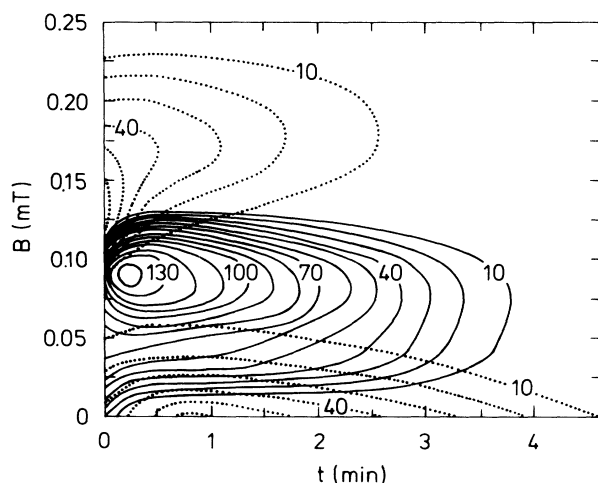


FIG. 3. The neutron intensity contour diagrams of the  $(\frac{1}{3}, \frac{1}{3})$  (solid line) and the (100) (dotted line) Bragg peaks as a function of time and external magnetic field. The outermost contours, 10 counts/sec, show approximately when long-range order disappears.

Fig. 4. The striking feature is the large size of the maximum intensity for the  $(\frac{1}{3}, \frac{1}{3})$  signal, compared to the weaker maxima of the (100) intensities.

There are twelve symmetry-related  $\mathbf{k}$  vectors for the  $(0, \frac{2}{3}, \frac{2}{3})$  and six for the (100) reflection. Comparing the intensity of the nuclear magnetic signal to the intensity of the nuclear peak observed at another wavelength and correcting for extinction, flux, and geometric effects, we can estimate the nuclear magnetic structure factor. This comparison is consistent, in the middle phase, with a spin structure characterized by the two vectors in the scattering plane:  $\mathbf{k}_1 = (2\pi/a)(0, \frac{2}{3}, \frac{2}{3})$  and  $\mathbf{k}_2 = (2\pi/a)(0, -\frac{2}{3}, -\frac{2}{3})$  alone. This implies a three-sublattice structure. After a similar comparison, the absolute neutron intensity observed in the uppermost phase is consistent with equal population of the three domains or a three- $\mathbf{k}$  structure.

During demagnetization through the uppermost and middle phases, domain formation could cause unequal distribution of the (100)-type regions at zero field. This might explain why the observed intensity at  $B=0$  is lower than expected. The time needed to establish equal distribution among the domains could be longer than the measuring time available. It is remarkable that the initial increase of the (100) signal at zero field is slower than any other transient effect seen in these experiments.

In conclusion, we have shown that scanning can be used, with some restrictions, for investigations of a spin system at nanokelvin temperatures. The commensurate ordering vector  $\mathbf{k} = (2\pi/a)(0, \frac{2}{3}, \frac{2}{3})$ , not observed in any electronic fcc antiferromagnet, was found in the ideal fcc nuclear-spin structure of copper. The intensities of the equivalent  $\pm(0, \frac{2}{3}, \frac{2}{3})$ ,  $(\frac{1}{3}, \frac{1}{3})$ , and  $(1 - \frac{1}{3} - \frac{1}{3})$  reflections and the (100) peak establish the presence of three antiferromagnetic phases as a function of the external magnetic field along the  $[01\bar{1}]$  direction. These results are in agreement with simultaneous susceptibility measurements.

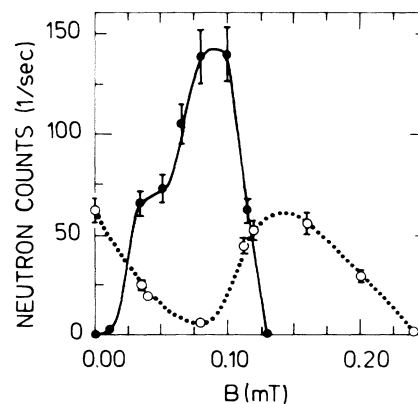


FIG. 4. Neutron intensities of the  $(\frac{1}{3}, \frac{1}{3})$  (●) and the (100) (○) reflections through the maxima of Fig. 3 as functions of the external magnetic field.

A clear first-order phase transition was found between the uppermost and the middle phases. The middle and the lowest phases appear to coexist over a wide field region, between  $B=0.02$  and  $0.07$  mT. In a narrow field range around  $0.03$  mT, the possibility of a two- $\mathbf{k}$  phase, with two different ordering vectors, cannot be ruled out. The discovery of the phase giving the  $(0 \frac{2}{3} \frac{2}{3})$  reflection does solve the puzzle of the previously missed neutron intensity<sup>6</sup> around  $B=0.10$  mT.

We thank Teppo Jyrkkö for valuable experimental advice. A.J.A. is indebted to the Cultural Foundation of Finland for scholarships and to the Magnus Ehrnrooth Foundation for travel funds. A.J.A. and O.V.L. acknowledge support by the Danish Research Academy. This work was partly funded by the Academy of Finland.

<sup>(a)</sup>Now at Institut für Physik, Johannes Gutenberg-Universität, D-6500 Mainz, Federal Republic of Germany.

<sup>1</sup>M. T. Huiku and M. T. Lojonen, Phys. Rev. Lett. **49**, 1288 (1982).

<sup>2</sup>M. T. Huiku, T. A. Jyrkkö, J. M. Kynnäräinen, A. S. Oja, and O. V. Lounasmaa, Phys. Rev. Lett. **53**, 1692 (1984).

<sup>3</sup>T. A. Jyrkkö, K. N. Clausen, M. T. Huiku, K. Kakurai, K. Siemensmeyer, and M. Steiner, Jpn. J. Appl. Phys. Suppl. **26-3**, 1717 (1987).

<sup>4</sup>H. Glättli and M. Goldman, in *Neutron Scattering*, edited by K. Sköld and D. L. Price, Methods of Experimental Physics Vol. 23 (Academic, New York, 1987), Pt. C, p. 241.

<sup>5</sup>M. Steiner, in *Neutron Scattering in the Nineties: Conference Proceedings, Jülich, West Germany, 14-18 January 1985* (International Atomic Energy Agency, Vienna, 1985), p. 185.

<sup>6</sup>T. A. Jyrkkö, M. T. Huiku, O. V. Lounasmaa, K.

Siemensmeyer, K. Kakurai, M. Steiner, K. N. Clausen, and J. K. Kjems, Phys. Rev. Lett. **60**, 2418 (1988).

<sup>7</sup>T. A. Jyrkkö, M. T. Huiku, K. Siemensmeyer, K. N. Clausen, J. Low Temp. Phys. **74**, 435 (1989).

<sup>8</sup>P.-A. Lindgård, X.-W. Wang, and B. N. Harmon, J. Magn. Mater. **545-57**, 1052 (1986).

<sup>9</sup>D. ter Haar and M. Lines, Philos. Trans. Roy. Soc. London **A 254**, 521 (1962); **255**, 1 (1962).

<sup>10</sup>P. W. Anderson, Mater. Res. Bull. **8**, 153 (1973).

<sup>11</sup>H. E. Viertiö and A. S. Oja, Phys. Rev. B **36**, 3805 (1987).

<sup>12</sup>P.-A. Lindgård, Phys. Rev. Lett. **61**, 629 (1988).

<sup>13</sup>S. J. Frisken and D. J. Miller, Phys. Rev. Lett. **61**, 1017 (1988).

<sup>14</sup>H. E. Viertiö and A. S. Oja, in *Quantum Fluids and Solids*, edited by G. G. Ihas and Y. Takano, AIP Conference Proceedings No. 194 (American Institute of Physics, New York, 1989).

<sup>15</sup>L. H. Kjälman and J. Kurkijärvi, Phys. Lett. **71A**, 454 (1979).

<sup>16</sup>M. A. Ruderman and C. Kittel, Phys. Rev. **96**, 99 (1954).

<sup>17</sup>E. R. Andrew, J. L. Carolan, and P. J. Randall, Phys. Lett. **37A**, 125 (1971).

<sup>18</sup>J. P. Ekström, J. F. Jacquinet, M. T. Lojonen, J. K. Soini, and P. Kumar, Physica (Amsterdam) **98B**, 451 (1979).

<sup>19</sup>P.-A. Lindgård, J. Phys. C **8**, 2051 (1988).

<sup>20</sup>A. S. Oja and P. Kumar, Physica (Amsterdam) **126B**, 451 (1984).

<sup>21</sup>A. S. Oja, X.-W. Wang, and B. N. Harmon, Phys. Rev. B **39**, 4009 (1989).

<sup>22</sup>P. J. Brown, Physica (Amsterdam) **137B**, 31-42 (1986).

<sup>23</sup>P.-A. Lindgård, H. E. Viertiö, and O. G. Mouritsen, Phys. Rev. B **38**, 6798 (1988).

<sup>24</sup>K. Siemensmeyer, K. Kakurai, M. Steiner, T. A. Jyrkkö, M. T. Huiku, and K. N. Clausen, in Proceedings of the Thirty-Fourth Conference on Magnetism and Magnetic Materials, Boston, 1989 [J. Appl. Phys. (to be published)].